# CHAPTER 3

# REDUCED LATTICE THERMAL CONDUCTIVITY OF Ti–SITE SUBSTITUTED TRANSITION METALS $Ti_{1-x}TM_xNiSn$: A QUASI–HARMONIC DEBYE MODEL STUDY

## Introduction

TiNiSn is a half Heusler alloy (Graf, Felser & Parkin, 2011), intermetallic (Zhu, Cheng & Schwingenschlögl, 2011), and having a narrow band gap (Gürth et al., 2016), which is suitable for an *n*–type thermoelectric (TE) material (Chaput, Tobola, Pécheur & Scherrer, 2006). The TE materials are considered by the dimensionless figure of merit: $ZT = S^2\sigma T/\kappa$. The main TE properties are composed of the Seebeck coefficient ($S$), the electrical conductivity ($\sigma$), and the thermal conductivity ($\kappa$), which are measured under an absolute temperature $T$ (Aswal, Basu & Singh, 2016). $\kappa$ includes the lattice term ($\kappa_{\mathrm{lat}}$) and the electron contribution term ($\kappa_{\mathrm{e}}$). $\kappa_{\mathrm{e}}$ is simply investigated as $\kappa_{\mathrm{e}} = L\sigma T$, where $L$ is the Lorenz number (Kittel, McEuen & McEuen, 1996). In order to improve the $ZT$, a high power factor ($PF = S^2\sigma$) and small $\kappa$ are required. Generally, TiNiSn has a high $S^2\sigma$, but it also has high $\kappa$, which directly affects to lower $ZT$ (Berry et al., 2017; Katayama, Kim, Kimura & Mishima, 2003; K. S. Kim et al., 2017; S.–W. Kim, Kimura & Mishima, 2007; Lkhagvasuren et al., 2017; Sakurada & Shutoh, 2005; Tang & Zhao, 2009). Katayama et al., (2003) have revealed that the $ZT$ was improved by reducing the $\kappa$ through Zr and Hf substituted on the Ti–site TiNiSn. Meanwhile, the Ni– and Sn–site required a small substitute–

concentration for reducing $\boldsymbol{\kappa}$. After that, several research groups have studied the $\boldsymbol{\kappa}$ of a transition metal (TM) substituted on the Ti–site TiNiSn, such as $Ti_{1-X}Zr_XNiSn$ (Katayama et al., 2003), $Ti_{1-X}Hf_XNiSn$ (Katayama et al., 2003), $Ti_{1-X}Zr_XHf_XNiSn$ (Sakurada & Shutoh, 2005; Tang & Zhao, 2009), $Ti_{1-X}Hf_XNiSn_{1-Z}Sb_Z$ (K. S. Kim et al., 2017; S.–W. Kim et al., 2007), $Ti_{1-X}Hf_XNi_{1-Y}(Pd, Pt)_YSn_{1-Z}Sb_Z$ (S.–W. Kim et al., 2007), $Ti_{1-X}Mn_XNiSn_{1-Z}Sb_Z$ (Berry et al., 2017), and $Ti_{1-X}Mn_XNiSn$ (Lkhagvasuren et al., 2017). By the way, the theoretical and experimental crystal structure for $Ti_{1-X}Sc_XNiSn$ (Bodak et al., 2004) and $Ti_{1-X}V_XNiSn$ (Stadnyk et al., 2010) were reported but the thermal properties and $\boldsymbol{\kappa}$ are lacking. Theoretically, the thermal properties including the lattice constant, bulk modulus, Grüneisen parameter, thermal expansion, and specific heat for TiNiSn and $TiNi_2Sn$ were investigated by the first–principles combined with quasi–harmonic approach (Hermet et al., 2014). Recently, the $\boldsymbol{\kappa}$ versus temperature for ShengBTE TiNiSn has been revealed by the quasi–harmonic Debye model (Toher et al., 2014) and the Boltzmann transport theory (Ding, Gao & Yao, 2015; Eliassen et al., 2017). Schrade *et al.*, (2017) have studied $\boldsymbol{\kappa}$ through the experimental data combined with the first–principles calculation. They showed that the $\boldsymbol{\kappa_{lat}}$ of the *X*NiSn system (*X* is Hf, Zr, and Ti) depends on $\boldsymbol{1/T}$. They found that the first–principles calculation has obtained a $\boldsymbol{\kappa}$ in good agreement with the experimental result. As mentioned above, several research groups have focused on the thermal properties and $\boldsymbol{\kappa}$ of TiNiSn. However, for the substitution case there are few studies and no complete fundamental treatment. Recently, we have successfully predicted the lattice thermal conductivity of lanthanide substitution on the Sr–site $SrTiO_3$ (Rittiruam et al., 2016). We demonstrated that the thermal properties can significantly improve the TE properties of $SrTiO_3$. In this work, we present a theoretical study on the thermal properties of Sc, Zr, Hf, V, Nb and Mn substituted on the Ti–site in the TiNiSn half Heusler alloy. We proposed to reduce the $\boldsymbol{\kappa_{lat}}$ of TiNiSn by TM substituted on the Ti–site. The density functional

theory and quasi-harmonic Debye model were employed to investigate the total energy, equation of state, Debye temperature, and Grüneisen parameter. The $\kappa_{lat}$ was calculated by using the Slack and Berman method.

## Computational details

The TM substitution on the Ti-site TiNiSn as the model $Ti_{1-X}TM_XNiSn$ (TM = Sc, Zr, Hf, V, Nb, Mn; X = 0, 0.25, 0.5, 0.75, 1.0) was designed by using the space group number 216 with the Wyckoff position of Ti(4a), Ni(4c) and Sn(4b). The total energies were calculated by the first-principles through the self-consistent field (SCF) based on the density functional theory (DFT) framework (Hohenberg & Kohn, 1964; Kohn & Sham, 1965). The kinetic energy cut-off of 40 Ry, convergence threshold of $1\times10^{-8}$ and mixing factor of 0.7 were used for the self-consistent calculation. We use the Perdew Burke Ernzerhof (Perdew, Burke & Ernzerhof, 1996) and generalized gradient approximation (Rappe, Rabe, Kaxiras & Joannopoulos, 1990) (PBE-GGA) for the exchange correlation function. The first Brillouin zone with 6×6×6 grid points was used for integration. The calculated energy-lattice curve was performed by the Quantum ESPRESSO package (P Giannozzi et al., 2017; Paolo Giannozzi et al., 2009). The equation of state (EOS) and thermal properties were calculated by the quasi-harmonic Debye model implemented in the GIBBS code (Blanco, Francisco & Luana, 2004). The theory of the Gibbs free energy as a quasi-harmonic Debye model has been successfully derived in Ref. (Blanco et al., 2004). The EOS was determined by using the Vinet (Vinet, Rose, Ferrante & Smith, 1989), Birch-Murnaghan (Poirier, 2000) and Spinoda l (Baonza, Cáceres & Núñez, 1995) as in the equations (Birch, 1947; Murnaghan, 1944)

$$V = V_0 \exp\left\{\frac{\beta}{(1-\beta)\mathrm{B}_0'}\right\} \exp\left\{\left[\left(\beta \frac{\mathrm{B}_0}{\mathrm{B}_0'}\right)^{\beta} \frac{1}{B_0(1-\beta)}\right]\left(p + \beta \frac{\mathrm{B}_0}{\mathrm{B}_0'}\right)^{1-\beta}\right\} \quad ; \quad \beta = 0.85 \ , \tag{62}$$

$$p = \frac{3}{2}\mathrm{B}_0 \left[\left(\frac{V_0}{V}\right)^{\frac{7}{3}} - \left(\frac{V_0}{V}\right)^{\frac{5}{3}}\right]\left\{1 + \frac{3}{4}(\mathrm{B}_0' - 4)\left[\left(\frac{V_0}{V}\right)^{\frac{2}{3}}\right] - 1\right\} \ , \tag{63}$$

$$\mathrm{B}_0 = -V\left(\frac{\partial p}{\partial V}\right)_{p=0} \quad ; \quad \mathrm{B}_0' = \left(\frac{\partial \mathrm{B}_0}{\partial p}\right)_{p=0} \ , \tag{64}$$

where $V_0$ is the volume and $\mathrm{B}_0$ is the bulk modulus at zero temperature and zero pressure, respectively. The thermal properties composed of the Debye temperature ($\Theta$), adiabatic bulk modulus ($\mathrm{B}_s$), isothermal bulk modulus ($\mathrm{B}_T$), Grüneisen parameter ($\gamma$), and volume thermal expansion ($\alpha$) were calculated with

$$\Theta = \frac{\hbar}{k_B}\left[6\pi^2 V^{\frac{1}{2}} n\right]^{\frac{1}{3}} \left\{3\left[2\left(\frac{2(1+\Sigma)}{3(1-2\Sigma)}\right)^{\frac{3}{2}} + \left(\frac{(1+\Sigma)}{3(1-\Sigma)}\right)^{\frac{3}{2}}\right]^{-1}\right\}^{1/3} \left(\frac{\mathrm{B}_S}{M}\right)^{1/2} \ , \tag{65}$$

$$\mathrm{B}_S = \mathrm{B}_T(1 + \alpha\gamma T) \ , \tag{66}$$

$$\mathrm{B}_T = -\left(\frac{V_0}{V}\right)^{\frac{2}{3}} \mathrm{B}_0 \left\{\left(\frac{V_0}{V}\right)^{\frac{1}{3}} - 2 - \frac{3}{2}(\mathrm{B}_0' - 1)\left[1 - \left(\frac{V_0}{V}\right)^{\frac{1}{3}}\right]\right\} \times \exp\left\{\frac{3}{2}(\mathrm{B}_0' - 1)\left[1 - \left(\frac{V_0}{V}\right)^{\frac{1}{3}}\right]\right\} \ , \tag{67}$$

$$\gamma = -\frac{\mathrm{d}\ln\Theta}{\mathrm{d}\ln V} \ , \tag{68}$$

$$\alpha = \frac{1}{V}\frac{\partial V}{\partial T} \ , \tag{69}$$

where $k_B$ is the Boltzmann constant, $\hbar$ is the Dirac constant, $n$ is number of atoms per formula, $M$ is the atomic mass per formula, and $T$ is the temperature, respectively. $\kappa_{\mathrm{lat}}$ was investigated by Slack (1979) and Berman (1976) using the Grüneisen parameter and Debye temperature, as in the equation

$$\kappa_{\mathrm{lat}} = A\frac{M_{av}\Theta^3 \mathrm{V}}{\gamma^2 T n^{2/3}} \ , \tag{70}$$

where $A$ is a constant, and $M_{av}$ is the average mass. Julian (1965) purposed the constant $A$ by using the Grüneisen parameter, as in the equation

$$A = \frac{2.43\times10^{-8}}{1-\left(\frac{0.514}{\gamma}\right)+\left(\frac{0.228}{\gamma^2}\right)} \quad . \tag{71}$$

Slack (1917) concluded $A$ is $3.04\times10^{-8}$ for $\gamma \approx 2$. Using equation (10) and (9), the $\kappa_{\mathrm{lat}}$ dependence on $\Theta$, $\gamma$ and $T$ can be expressed as

$$\kappa_{\mathrm{lat}}(\Theta,\gamma,T) = \left(\frac{2.43\times10^{-8}}{\gamma^2-\gamma(0.514)+(0.228)}\right)\frac{M_{av}\Theta^3\mathrm{V}}{Tn^{2/3}} \quad . \tag{72}$$

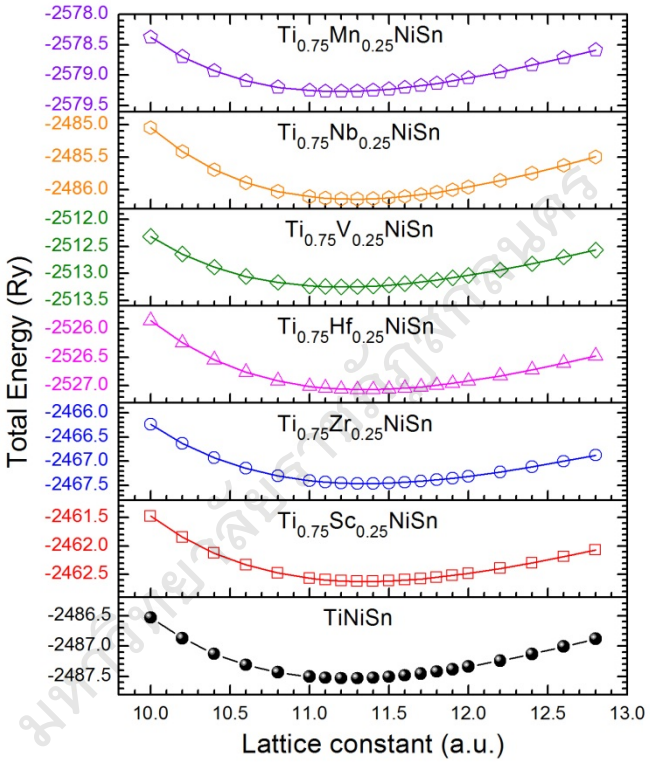


Figure 17 The total energies versus lattice constant for $Ti_{0.75}TM_{0.25}NiSn$ (TM = Sc, Zr, Hf, V, Nb, Mn).

## Results and Discussion

The calculated results of the energy–lattice for the composition X equal to 0.25, 0.5, 0.75, and 1 exhibit a U–curve. Then, we present the calculated energy–lattice curve of $Ti_{0.75}TM_{0.25}NiSn$ as shown in Figure 17.

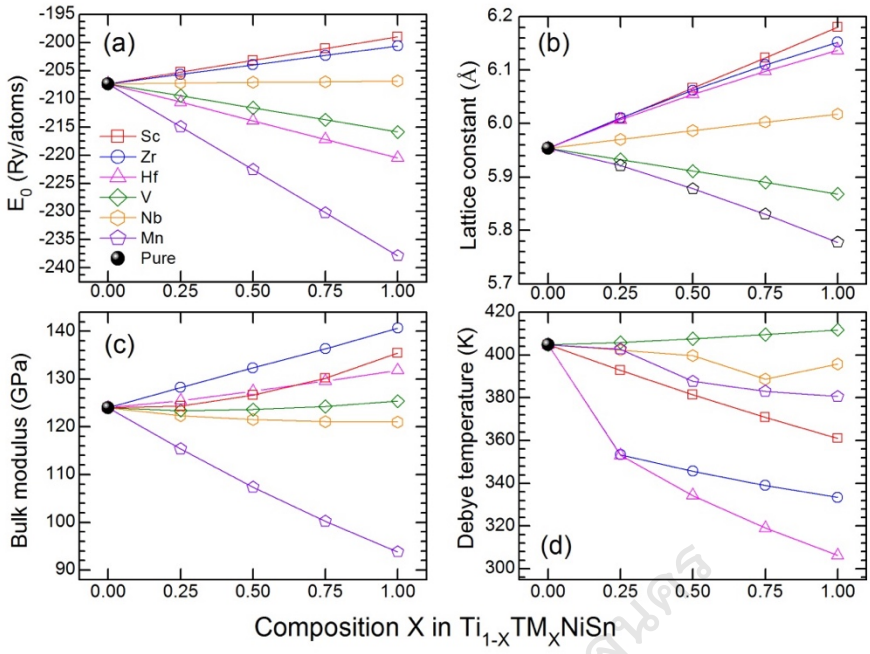


Figure 18 The minimum total energies (a), lattice constant (b), bulk modulus (c), and Debye temperature (d) for $Ti_{1-X}TM_XNiSn$ (TM = Sc, Zr, Hf, V, Nb, Mn) at the ground state.

The minimum total energy ($\mathbf{E_{tot}}$) of $Ti_{1-X}TM_XNiSn$ is illustrated in Figure 18(a). The calculated $\mathbf{E_{tot}}$ is –207.29 Ry/atoms for TiNiSn, it decreased with the substitution by Sc and Zr, while Hf, V, and Mn exhibit $\mathbf{E_{tot}}$ more than TiNiSn. In addition, $\mathbf{E_{tot}}$ showed slightly different values with substitution by Nb. The calculated $a_0$ is 5.9536 Å for TiNiSn, while the experimental data is around 5.9400 Å (Cook & Harringa, 1999; Hermet et al., 2014; Jeitschko, 1970; Jung, Kurosaki, Kim, Muta & Yamanaka, 2010). However, our calculated $a_0$ is in good agreement with the PBE–GGA approximation (Kirievsky, Shlimovich, Fuks & Gelbstein, 2014; Wang et al., 2009). From Figure 18(b), $a_0$ increased with substitution by Sc, Zr, and Hf, but it decreased with substitution by V and Mn. The different results of $a_0$ can be expressed by the calculated atomic radius (Clementi, Raimondi & Reinhardt, 1967) such as, 176 pm for Ti, 184 pm for Sc, 206 pm for Zr, 208 pm Hf, 171 pm for V, and 161 pm for Mn. From Figure 18(c), our calculated $\mathbf{B_0}$ is 124.01 GPa for TiNiSn, which agrees with

the experimental (Colinet, Jund & Tédenac, 2014) and theoretical (Kirievsky et al., 2014; Li et al., 2016) values. The calculated $a_0$ and $B_0$ together with the experimental and theoretical data are presented in Table 4.

Table 4 The lattice constant ($a_0$) and bulk modulus ($B_0$) of $Ti_{1-X}TM_XNiSn$ (TM = Sc, Zr, Hf, V, Nb, Mn) together with the experimental and theoretical data.

| $Ti_{1-X}TM_XNiSn$ | $a_0$ (Å) | | $B_0$ (GPa) | |
|---|---|---|---|---|
| | This work | References | This work | References |
| TiNiSn | 5.9536 | 5.94[a] (Cook & Harringa, 1999; Jeitschko, 1970), 5.939[a] (Jung et al., 2010), 5.9419[a] (Hermet et al., 2014) 5.95[b] (Kirievsky et al., 2014; Wang et al., 2009) | 124.01 | 121[a] (Colinet et al., 2014), 128[b] (Kirievsky et al., 2014; Li et al., 2016) |
| $Ti_{0.75}Sc_{0.25}NiSn$ | 6.0095 | 5.9932[b] (X=0.20) (Romaka et al., 2005), | 115.34 | |
| $Ti_{0.50}Sc_{0.50}NiSn$ | 6.0660 | 6.0212[b] (X=0.30) (Romaka et al., 2005), | 107.38 | |
| $Ti_{0.25}Sc_{0.75}NiSn$ | 6.1229 | 6.0302[b] (X=0.40) (Romaka et al., 2005), | 100.22 | |
| ScNiSn | 6.1802 | 6.0302[b] (X=0.50) (Romaka et al., 2005), 6.1092[b] (X=0.60) (Romaka et al., 2005), 6.1860[b] (ScNiSn) (Xie et al., 2012) | 93.80 | |
| $Ti_{0.75}Zr_{0.25}NiSn$ | 6.0105 | 6.1443[a] (ZrNiSn) (Slebarski et al., 2000), | 122.36 | |
| $Ti_{0.50}Zr_{0.50}NiSn$ | 6.0621 | 6.1098[a] (ZrNiSn) (Larson, Mahanti & | 121.51 | |
| $Ti_{0.25}Zr_{0.75}NiSn$ | 6.1095 | Kanatzidis, 2000), 6.1111[a] (ZrNiSn) (Xie et | 121.07 | |
| ZrNiSn | 6.1523 | al., 2012), 6.162[b] (ZrNiSn) (Zou, Xie, Liu, Lin & Li, 2013), 6.154[b] (ZrNiSn) (Miyazaki et al., 2014) | 121.04 | |
| $Ti_{0.75}Hf_{0.25}NiSn$ | 6.0071 | 6.0601[b] (X=0.50) (Chaput et al., 2006), | 123.42 | |
| $Ti_{0.50}Hf_{0.50}NiSn$ | 6.0548 | 6.1236[a] (HfNiSn) (Xie et al., 2012), 6.113[b] | 123.61 | |
| $Ti_{0.25}Hf_{0.75}NiSn$ | 6.0980 | (HfNiSn) (Page et al., 2015) | 124.28 | |
| HfNiSn | 6.1369 | | 125.39 | |
| $Ti_{0.75}V_{0.25}NiSn$ | 5.9324 | 5.9310[a] (X=0.10) (Stadnyk et al., 2010) | 125.51 | |
| $Ti_{0.50}V_{0.50}NiSn$ | 5.9111 | | 127.44 | |
| $Ti_{0.25}V_{0.75}NiSn$ | 5.8898 | | 129.56 | |
| VNiSn | 5.8682 | | 131.84 | |
| $Ti_{0.75}Nb_{0.25}NiSn$ | 5.9702 | | 128.26 | |
| $Ti_{0.50}Nb_{0.50}NiSn$ | 5.9871 | | 132.32 | |
| $Ti_{0.25}Nb_{0.75}NiSn$ | 6.0030 | | 136.37 | |
| NbNiSn | 6.0180 | | 140.69 | |
| $Ti_{0.75}Mn_{0.25}NiSn$ | 5.9216 | | 124.36 | |
| $Ti_{0.50}Mn_{0.50}NiSn$ | 4.8782 | | 126.65 | |
| $Ti_{0.25}Mn_{0.75}NiSn$ | 5.8306 | | | |
| MnNiSn | 5.7778 | | 130.21 | |

[a] experimental data, [b] theoretical data

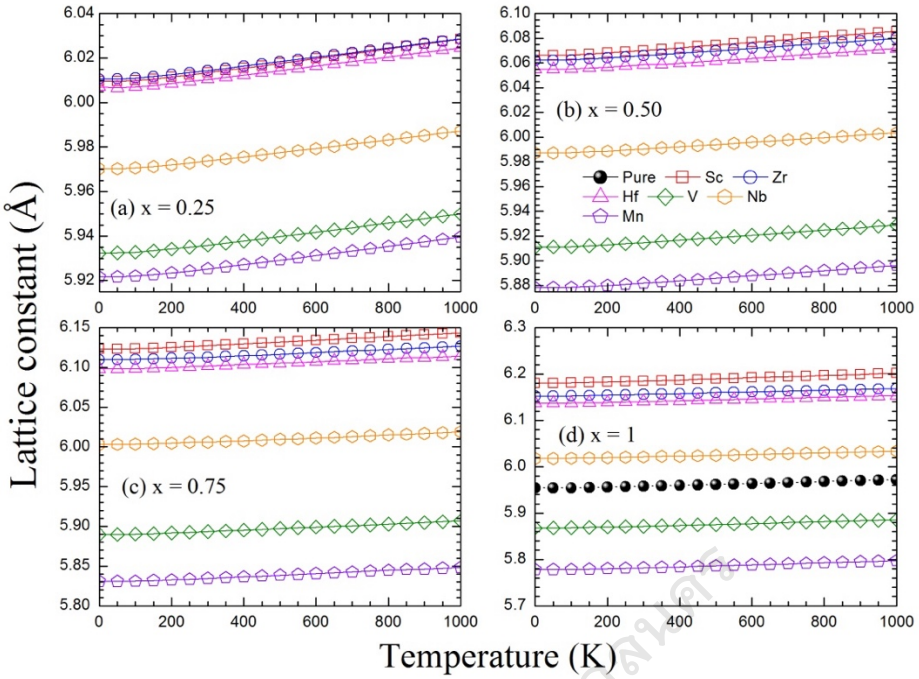


Figure 19 The lattice constant versus temperature for $Ti_{1-X}TM_XNiSn$ (TM = Sc, Zr, Hf, V, Nb, Mn; X = 0 – 1).

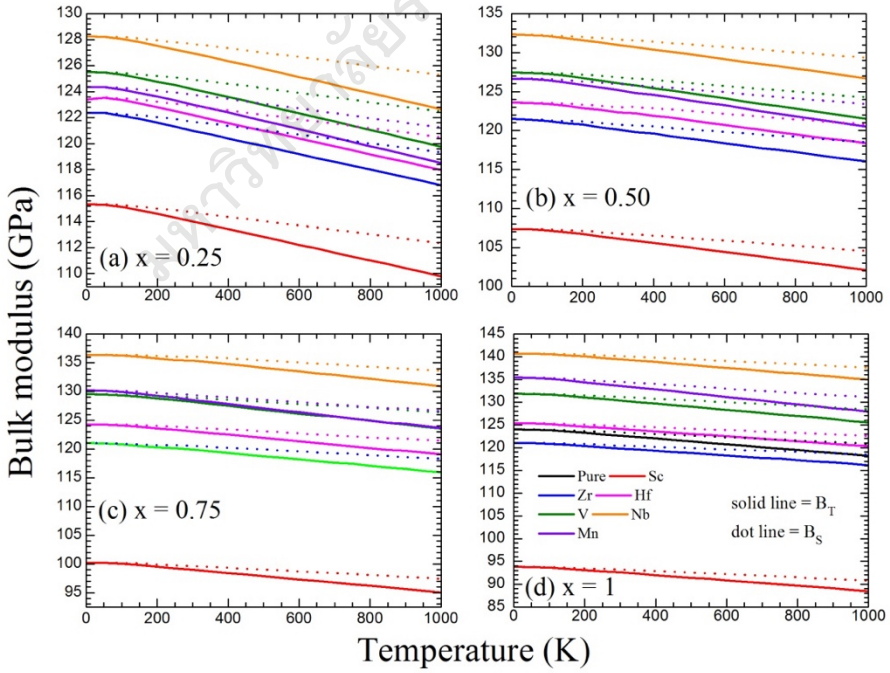


Figure 20 The bulk modulus versus temperature for $Ti_{1-X}TM_XNiSn$ (TM = Sc, Zr, Hf, V, Nb, Mn; X = 0 – 1).

Table 5 The Debye temperature (Θ) of $Ti_{1-X}TM_XNiSn$ (TM = Sc, Zr, Hf, V, Nb, Mn) together with the experimental and theoretical data at 300 K.

| $Ti_{1-X}TM_XNiSn$ | Θ (K) | |
|---|---|---|
| | This work | References |
| TiNiSn | 404.86 | 407[a] (Kuentzler et al., 1992), 415[b] (Kirievsky et al., 2014), 359 [b](Toher et al., 2014), 370 [b] (Page et al., 2015) |
| $Ti_{0.75}Sc_{0.25}NiSn$ | 392.89 | |
| $Ti_{0.50}Sc_{0.50}NiSn$ | 381.89 | |
| $Ti_{0.25}Sc_{0.75}NiSn$ | 370.84 | |
| ScNiSn | 361.13 | |
| $Ti_{0.75}Zr_{0.25}NiSn$ | 353.37 | 323[a] (ZrNiSn) (Kuentzler et al., 1992), 372[b] (ZrNiSn) (Page et al., 2015) |
| $Ti_{0.50}Zr_{0.50}NiSn$ | 345.69 | |
| $Ti_{0.25}Zr_{0.75}NiSn$ | 339.05 | |
| ZrNiSn | 333.39 | |
| $Ti_{0.75}Hf_{0.25}NiSn$ | 353.05 | 307[a] (HfNiSn) (Kuentzler et al., 1992), 332[b] (HfNiSn) (Toher et al., 2014), 320[b] (HfNiSn) (Page et al., 2015) |
| $Ti_{0.50}Hf_{0.50}NiSn$ | 334.36 | |
| $Ti_{0.25}Hf_{0.75}NiSn$ | 319.12 | |
| HfNiSn | 306.32 | |
| $Ti_{0.75}V_{0.25}NiSn$ | 405.88 | |
| $Ti_{0.50}V_{0.50}NiSn$ | 407.61 | |
| $Ti_{0.25}V_{0.75}NiSn$ | 409.55 | |
| VNiSn | 411.82 | |
| $Ti_{0.75}Nb_{0.25}NiSn$ | 402.41 | |
| $Ti_{0.50}Nb_{0.50}NiSn$ | 399.82 | |
| $Ti_{0.25}Nb_{0.75}NiSn$ | 388.77 | |
| NbNiSn | 395.84 | |
| $Ti_{0.75}Mn_{0.25}NiSn$ | 402.77 | |
| $Ti_{0.50}Mn_{0.50}NiSn$ | 387.74 | |
| $Ti_{0.25}Mn_{0.75}NiSn$ | 383.02 | |
| MnNiSn | 380.60 | |

[a] experimental data, [b] theoretical data

Table 6 The lattice thermal conductivity ($\kappa_{lat}$ in W $m^{-1}$ $K^{-1}$) of $Ti_{1-X}TM_XNiSn$ (TM = Sc, Zr, Hf, V, Nb, Mn) together with the literature values which are present at 300 K.

| $Ti_{1-X}TM_XNiSn$ | $\kappa_{lat}$ (W $m^{-1}$ $K^{-1}$) | |
|---|---|---|
| | This work | References |
| TiNiSn | 9.23 | 7.50[a] (Hohl et al., 1999), 10.70[a] (Bhattacharya et al., 2008), 7.00[a] (Toher et al., 2014), 6.00[b] (Katayama et al., 2003), 8.00[b] (Muta, Kanemitsu, Kurosaki & Yamanaka, 2009), 7.60[b] (Lkhagvasuren et al., 2017), 13.80[c] (Ding et al., 2015), 6.00[c] (Eliassen et al., 2017) |
| $Ti_{0.75}Sc_{0.25}NiSn$ | 8.78 | |
| $Ti_{0.50}Sc_{0.50}NiSn$ | 8.36 | |
| $Ti_{0.25}Sc_{0.75}NiSn$ | 7.93 | |
| ScNiSn | 7.51 | |
| $Ti_{0.75}Zr_{0.25}NiSn$ | 6.72 | 10.22[a] (X = 0.1) (Hohl et al., 1999), 8.80[a] (X = 1.0) (Hohl et al., 1999), 5.00[a] (X = 0.1) (Toher et al., 2014), 10.10[c] (Schrade et al., 2017) (X = 1.0), 6.80[b] (X = 1.0) (Muta, Kanemitsu, Kurosaki & Yamanaka, 2006), 15.80[c] (X = 0.1) (Ding et al., 2015), 7.60[c] (X = 0.1) (Eliassen et al., 2017), 5.00[c] (X = 0.5) (Eliassen et al., 2017) |
| $Ti_{0.50}Zr_{0.50}NiSn$ | 6.82 | |
| $Ti_{0.25}Zr_{0.75}NiSn$ | 6.98 | |
| ZrNiSn | 7.06 | |
| $Ti_{0.75}Hf_{0.25}NiSn$ | 7.36 | 12.97[a] (X = 1.0) (Bhattacharya et al., 2008), 6.70[a] (X = 1.0) (Hohl et al., 1999), 5.20[a] (X = 0.05) (Toher et al., 2014), 4.00[a] (X = 0.1) (Toher et al., 2014), 3.80[a] (X = 0.2) (Toher et al., 2014), 3.70[a] (X = 0.5) (Toher et al., 2014), 12.00[a] (X = 1.0) (Uher, Yang, Hu, Morelli & Meisner, 1999), 6.30[b] (X = 1.0) (Liu et al., 2015) |
| $Ti_{0.50}Hf_{0.50}NiSn$ | 7.35 | |
| $Ti_{0.25}Hf_{0.75}NiSn$ | 7.34 | |
| HfNiSn | 7.33 | |
| $Ti_{0.75}V_{0.25}NiSn$ | 9.19 | |
| $Ti_{0.50}V_{0.50}NiSn$ | 9.13 | |
| $Ti_{0.25}V_{0.75}NiSn$ | 9.07 | |
| VNiSn | 9.08 | |
| $Ti_{0.75}Nb_{0.25}NiSn$ | 9.60 | 6.60[b] (X = 0.01) (Katayama et al., 2003), 7.00[b] (X = 0.02) (Katayama et al., 2003), 6.80[b] (X = 0.05) (Katayama et al., 2003) |
| $Ti_{0.50}Nb_{0.50}NiSn$ | 9.82 | |
| $Ti_{0.25}Nb_{0.75}NiSn$ | 9.47 | |
| NbNiSn | 10.46 | |
| $Ti_{0.75}Mn_{0.25}NiSn$ | 8.86 | 7.40[b] (X = 0.03) (Muta et al., 2009), 4.70[b] (X = 0.1) (Muta et al., 2009), 5.40[b] (X = 0.2) (Muta et al., 2009) |
| $Ti_{0.50}Mn_{0.50}NiSn$ | 7.60 | |
| $Ti_{0.25}Mn_{0.75}NiSn$ | 7.06 | |
| MnNiSn | 6.66 | |

[a] steady-state (experimental data), [b] laser flash (experimental data), [c] phonon Boltzmann transport equation (theoretical data)

The calculated lattice constant versus temperature appears in Figure 19. The temperature dependency on the lattice constant of TiNiSn, ZrNiSn, and HfNiSn are in good agreement with the experimental results of Slebarski et al. (2000), Jung et al. (2000), and the theoretical results of Hermet et al. (2014), respectively. It can be observed that the structure has expanded with increasing temperature due to the lattice constant having increased. In Figure 20, $\mathbf{B_T}$ decreased with increasing temperature due to it depending on $\mathbf{1/V}$. In addition, $\mathbf{B_T}$ has slightly decreased with substitution by Sc, while another sample has quickly decreased with increasing temperature. The bulk modulus decreased with increasing temperature for TiNiSn, in agreements with the theoretical data (Hermet et al., 2014).

The calculated $\Theta$ and $\boldsymbol{\kappa_{lat}}$ at 300 K for $Ti_{1-X}TM_XNiSn$ together with the literature values are presented in Tables 5 and 6. The calculated $\Theta$ is 404.86 K for TiNiSn, 333.39 K for ZrNiSn, and 306.32 K for HfNiSn, which agrees with the experimental and theoretical data (Kirievsky et al., 2014; Kuentzler, Clad, Schmerber & Dossmann, 1992; Page, Uher, Poudeu & Van der Ven, 2015; Toher et al., 2014). From Figure 18(d), the calculated $\Theta$ increased with substitution by V, but the Sc, Zr, Hf, Nb, and Mn show a $\Theta$ less than TiNiSn. The calculated $\Theta$ exhibits a value decreased with increasing temperature as shown in Figure 21. The calculated $\Theta$ combined with $V$ yields $\gamma$, as shown in Figures 22(a) and 22(c).

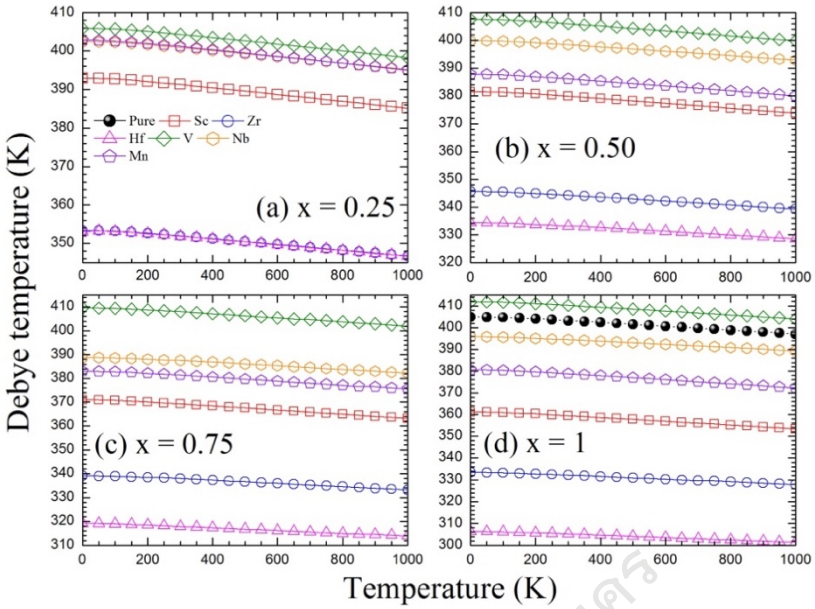


Figure 21 The Debye temperature versus temperature for $Ti_{1-X}TM_XNiSn$ (TM = Sc, Zr, Hf, V, Nb, Mn; X = 0 – 1).

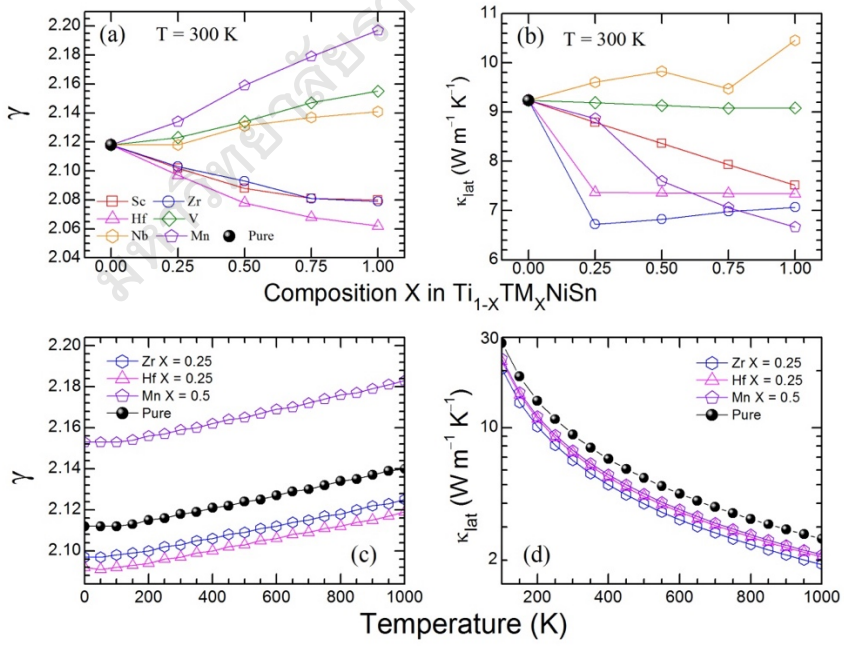


Figure 22 The Grüneisen parameter (a) and lattice thermal conductivity (b) for $Ti_{1-X}TM_XNiSn$ (TM = Sc, Zr, Hf, V, Nb, Mn; X = 0 – 1). The Grüneisen parameter (c) and lattice thermal conductivity (d) versus temperature for $Ti_{0.75}Zr_{0.25}NiSn$, $Ti_{0.75}Hf_{0.25}NiSn$, and $Ti_{0.50}Mn_{0.50}NiSn$.

The calculated $\gamma$ of V and Nb are slightly different from that of TiNiSn at composition X = 0.25. The $\gamma$ of TiNiSn has been reduced with substitution by Sc, Zr, and Hf, while it increased when substituted by V, Nb, and Mn. From Table 6, the calculated $\kappa_{lat}$ of TiNiSn is 9.23 W $m^{-1}$ $K^{-1}$ at 300 K, in good agreement with the literature. $\kappa_{lat}$ shows an increase with substitution by Nb, but V exhibits a constant $\kappa_{lat}$, as shown in Figure 22(b). In order to describe why $\kappa_{lat}$ is decreased with the substitution of Sc, Zr, Hf and Mn, we refer to equations (71) and (72). At constant temperature, the involved parameters of $\kappa_{lat}(\Theta, \gamma, T)$ include $\Theta$, $\gamma$, V, and $M_{av}$. The $\gamma$ in Figure 22(a) shows a small difference value on the order of $10^{-2}$. From equation (10), the constant $A$ is about $3.04\times10^{-8}$ for $\gamma \approx 2$. V was used in the unit $Å^3$ by Slack (Slack, 1979) and Berman (Berman, 1976). Besides, we obtained a large value of $\Theta^3$, on the order ~2.7×$10^7$ – ~7.3×$10^7$ $K^3$. We compared the value of each parameter in equation (72) and found that the $\gamma$ and V have a small effect on $\kappa_{lat}(\Theta, \gamma, T)$. So $\Theta$ is an important parameter for $\kappa_{lat}(\Theta, \gamma, T)$. From the periodic table of elements, in addition, the atomic mass shows Hf(178 amu) more than Nb(92.91 amu), Zr(91.22 amu), Mn(54.94 amu), V(50.94 amu), Ti(47.88 amu), and Sc(44.96 amu), respectively. In the case of a heavy atom substitution, $Ti_{1-X}Hf_XNiSn$ shows a value of $\Theta$ less than of TiNiSn which contributes to decreasing $\kappa_{lat}$. In addition, the $\kappa_{lat}$ of V and Nb are more than that of TiNiSn due to the atomic mass of V and Nb being more than that of Ti.

The good TE performance for TiNiSn can be enhanced by Sc, Zr, Hf, and Mn through the reducing $\kappa_{lat}$. It can be observed that the $\kappa_{lat}$ of Zr (X = 0.25), Hf (X = 0.25), and Mn (X = 0.5) have good potential for TM substitution on the Ti–site. The $\gamma$ and $\kappa_{lat}$ of $Ti_{0.75}Zr_{0.25}NiSn$, $Ti_{0.75}Hf_{0.25}NiSn$, and $Ti_{0.50}Mn_{0.50}NiSn$ were plotted versus temperature, as shown in Figure 22(c) and 22(d). The calculated $\kappa_{lat}$ is 2.59 W $m^{-1}$ $K^{-1}$ for TiNiSn, 1.89 W $m^{-1}$ $K^{-1}$ for $Ti_{0.75}Zr_{0.25}NiSn$, 2.08 W $m^{-1}$ $K^{-1}$ for $Ti_{0.75}Hf_{0.25}NiSn$, and

2.13 W $m^{-1}$ $K^{-1}$ for $Ti_{0.50}Mn_{0.50}NiSn$ at 1000 K, respectively. Therefore, a small $\kappa_{lat}$ at 1000 K has implied that the TE performance has increased.

## Summary

The quasi–harmonic Debye model was used to calculate the structural and thermal properties of TM substitution on the Ti–site in TiNiSn for the model $Ti_{1-x}TM_xNiSn$ (TM = Sc, Zr, Hf, V, Nb and Mn). The TM reduced $\kappa_{lat}$ of TiNiSn is proposed. It was revealed that the structure of TiNiSn was perturbed with substitution by the TM. In thermal properties, the Sc, Zr, Hf, Nb, and Mn have the effect of reducing the Debye temperature. While the $\kappa_{lat}$ of TiNiSn was reduced with substitution by Sc, Zr, Hf, and Mn. The $\kappa_{lat}$ of TiNiSn was reduced by 17.65 – 27.19% for $Ti_{0.75}Zr_{0.25}NiSn$, $Ti_{0.75}Hf_{0.25}NiSn$, and $Ti_{0.50}Mn_{0.50}NiSn$, which has good potential for enhancing the thermoelectric properties of the TiNiSn–based half Heusler alloy.